Am J Cancer Res 2023;13(8):3781-3798
www.ajcr.us /ISSN:2156-6976/ajcr0151091

Original Article

Carcinogen-induced super-enhancer RNA promotes nasopharyngeal carcinoma metastasis through NPM1/c-Myc/NDRG1 axis

Qunying Jia[1], Hongyu Deng[1], Yao Wu[1,2], Yingchun He[2], Faqin Tang[1]

[1]*Hunan Key Laboratory of Oncotarget Gene and Clinical Laboratory of Hunan Cancer Hospital, The Affiliated Cancer Hospital of Xiangya School of Medicine, Central South University, Changsha 410013, Hunan, China;* [2]*Hunan University of Chinese Medicine, Changsha 410208, Hunan, China*

Received May 5, 2023; Accepted August 6, 2023; Epub August 15, 2023; Published August 30, 2023

Abstract: Chemical carcinogen is one etiology of nasopharyngeal carcinoma (NPC) occurrence, N,N'-Dinitrosopiperazine (DNP) has been verified to cause NPC cell metastasis and generate induced pluripotent stem cells (iPSCs). To investigate the oncogenic mechanism of DNP, NPC cells were exposed to DNP, and subjected to RNA-seq, GRO-seq, ChIP-seq, and data analysis. The results showed that the super-enhancer RNA (seRNA) participates in DNP-mediated NPC metastasis through regulating N-myc downstream regulated gene 1 (NDRG1). Mechanistically, DNP exposure upregulates the levels of NPC metastatic seRNA (seRNA-NPCm), seRNA-NPCm interacted with a special super-enhancer (SE) upstream of NDRG1 gene and bound to nucleophosmin (NPM1)/c-Myc complex at the NDRG1 promoter, resulting in an increase of NDRG1 transcription. Functional studies showed that DNP significantly increased the metastatic capability of NPC cells in vitro and in vivo. Knockdown of seRNA-NPCm in NPC cells impaired the capability of metastasis. Furthermore, stably overexpressing seRNA-NPCm significantly increased the metastatic ability of NPC cells, while restoration of NDRG1 levels in these cells restored their metastatic capacity. Finally, the immunohistochemistry and in situ hybridization analyses revealed that the expression of seRNA-NPCm in NPC patients is positively correlated with NDRG1, and the NDRG1 level independently predicts poor prognosis of NPC patients. Collectively, DNP induces seRNA-NPCm, and seRNA-NPCm promotes NPC metastasis through NPM1/c-Myc/NDRG1 axis.

Keywords: Metastasis, nasopharyngeal carcinoma, R-loop, SE-promoter looping, seRNA

Introduction

Nasopharyngeal carcinoma (NPC) is a common malignancy mainly occurring in South China and Southeast Asia [1]. Advanced-stage NPC patients have very poor prognoses mainly due to local recurrence and distant metastasis [2]. Chemical carcinogens exposure and certain dietary habits might be two key etiology factors in NPC oncogenesis and metastasis [3, 4]. High intakes of nitrosamines during childhood were associated with increased risk of NPC [5]. N,N'-Dinitrosopiperazine (DNP) is a predominant volatile nitrosamine enriched in preserved foods [6], and has been shown to induce NPC carcinogenesis and metastasis in vivo and in vitro [7]. The previous reports revealed that DNP may promote NPC metastasis via regulation of AGR2 [8], HSP70 [9], and Clusterin [10]. However, the exact mechanism of NPC metastasis is not clear.

As a type of regulatory elements, enhancers are DNA fragments which often modulate target gene expression by forming chromatin loops with promoters [11]. Super-enhancers (SEs) are clusters of enhancers with high levels of histone H3 lysine 27 acetylation (H3K27ac), transcription factors (TFs), and co-factors [12]. Active SEs occupied by RNA polymerase II (RNAP II) can either bidirectionally or unidirectionally transcribe into super-enhancer RNAs (seRNAs) [13]. eRNAs/seRNAs may not only bind protein partners, but also DNAs directly to modulate enhancer/SE function. The nascent RNA transcripts hybridize with DNAs to form

special three-stranded nucleic acid structure, named as R-loop, to involve in genomic instability [14]. Increased seRNA led to R-loop formation and consequent genomic instability at SEs [15]. A few recent works showed that global enhancer was activated in most cancers [16], and dysregulated seRNAs have been causally linked to tumorigenesis [17].

N-myc downstream regulated gene 1 (NDRG1) is a stress response protein that is involved in the cell proliferation, differentiation, migration, and invasion [18, 19]. The overexpression of NDRG1 is induced by hypoxia in various cancers, such as liver cancer, lung cancer, and brain cancer [20]. NDRG1 downregulation in human hepatocellular carcinoma (HCC) resulted in cell apoptosis by increase of BAX and decrease in Bcl-2 and Bclx [21]. Upregulated NDRG1 promoted stemlike properties of NSCLC cells including induced pluripotent stem cell (iPSC) factors c-Myc through Skp2-mediated ubiquitination [22]. In bladder cancer, NDRG1 overexpression facilitated disease progression by influencing the epithelial-to-mesenchymal transition (EMT) process [23]. NDRG1 also inhibited cell proliferation and invasion, playing an anti-oncogenic and anti-metastatic role in cancers [24-27]. The role of NDRG1 on NPC cells was rarely studied so far. A previous study showed that NDRG1 downregulation could promote NPC cells tumorigenesis and migration by facilitating Smad2-mediated EMT process [28]. Further studies are needed to elucidate the biological functions of NDRG1 in NPC pathogenesis.

In this study, we identified a special seRNA, named seRNA-NPCm, as an important transcriptional regulator involved in DNP-mediated metastasis in NPC cells. Our results showed that DNP induced the expression of seRNA-NPCm, accompanied by the elevation of NDRG1. seRNA-NPCm bound to nucleophosmin (NPM1)/c-Myc at the promoter of NDRG1, and the hybridization with SE 41.8 Kb upstream of NDRG1 facilitated chromatin looping, leading to NDRG1 transcription. In addition, DNP promoted metastasis of NPC cells in vitro and in vivo. The expression of seRNA-NPCm in NPC patients is positively correlated with NDRG1, and NDRG1 is an independent prognostic factors for NPC patients. Taken together, the results in this study indicated that seRNA-NPCm may serve as a novel target for NPC therapy and diagnosis, and we reported a new spatiotemporal conformational interaction between SE and promoters through seRNAs in DNP-mediated NPC.

Materials and methods

Cell culture and stable cell lines

Human NPC cell lines (S18, S26, 6-10B, 5-8F) were obtained from the Institute of Biochemistry and Cell Biology of the Chinese Academy of Sciences (Shanghai, China). All cells were cultured in RPMI 1640 media (Thermo Fisher, MA) supplemented with 10% fetal bovine serum (FBS) and 100 U/ml Penicillin-Streptomycin (P/S). All cell lines were mycoplasma-free and detected by short tandem repeat (STR) analysis before the experiments. To generate stably expressing cells, the lentiviral particles purchased from Genechem (Shanghai, China) were used to infect NPC cells for 12 h. After 48 h of puromycin (5 μg/mL) selection, the cells were harvested and the target mRNA expression was confirmed by quantitative PCR (q-PCR). shRNA sequences are included in Supplementary Data 3.

Antibodies

The following antibodies were used for Western blot or for ChIP analysis: rabbit anti-NDRG1 monoclonal antibody (ab124689, Abcam), rabbit anti-c-Myc monoclonal antibody--ChIP Grade (ab32072, Abcam), mouse anti-c-Myc monoclonal antibody (SANTA Cruz Biotechnology, USA), mouse anti-NPM1 monoclonal antibody (32-5200, Thermo Fisher), rabbit anti-E-Cadherin monoclonal antibody (3195, Cell Signaling Technology), rabbit anti-N-Cadherin monoclonal antibody (13116, Cell Signaling Technology), rabbit anti-snail monoclonal antibody (3879, Cell Signaling Technology), rabbit anti-vimentin monoclonal antibody (5741, Cell Signaling Technology), mouse anti-GAPDH antibody (60004-1-Ig, proteintech), HRP-conjugated goat anti-rabbit IgG (SA00001-2, proteintech), HRP-conjugated goat anti-mouse IgG (SA00001-1, proteintech).

Quantitative PCR

Total RNA extraction was performed by the Total RNA Kit II reagent following the manufacturer's instructions (Omega, USA). Nuclear and cytoplasmic RNA extractions were obtained

using the Cytoplasmic and Nuclear RNA purification Kit according to the manufacturer's instructions (Norgen Biotek Corp., CA, USA). Quantitative PCR was performed by LightCycler® 480 Instrument II System (Roche Life Science). The relative RNA expression levels were quantified by the $2^{-\Delta\Delta Ct}$ method, with GAPDH as the internal control. The primers used in these analyses are listed in Supplementary Data 3.

Mouse experiment

All animal studies were approved by the Institutional Animal Care and Use Committee of the Hunan Cancer Hospital. Female BALB/c nude mice (4-6 weeks) were purchased from Hunan SJA Laboratory Animal Co. (Changsha, China) and cultured in specific pathogen-free room, with free access to food and water and in a 12-hour light-dark cycle. The nude mice were randomly allocated into different groups. In assays to detect single NPC cell RNA levels, 1×10^6 cells of S26 and S26-DNP were injected into tail veins of mice, where S26-DNP cells were S26 cells treated with 200 μM DNP for a week. Subcutaneous metastases were harvested for single-cell RNA sequencing 4 weeks later. In the measurement of lung metastasis formation, 1×10^6 cells of luciferase-labeled NPC cells were injected into tail veins of mice. The pulmonary metastases were monitored by ex vivo bioluminescence imaging (AniView100 Imaging System, China). When the mice exhibited the following humane-endpoint: significant body weight loss, prostration, rotational motion, difficulty breathing, and body temperature drop, they were humanely sacrificed by inhalation of 30% vol/min CO_2.

CRISPR interference

CRISPR interference was performed as previously reported [29]. Two pairs of guide RNAs (gRNAs) were designed to target 1816 bp region upstream of NDRG1. Lentiviral vectors expressing gRNAs and Cas9 mRNA were purchased from Genechem (Shanghai, China). Primers for CRISPR interference are listed in Supplementary Data 3.

RACE assay

The RACE assay was performed as previously reported [30]. To analysis the 5' and 3' ends sequences of seRNA-NPCm, GeneRacer™ Kit (Invitrogen, L1500-01) was applied according to the manufacturer's instructions. The primers for RACE analysis are listed in Supplementary Data 3.

RNA pull-down and MS assays

RNA pull-down assay was performed as previously reported [31]. Briefly, biotin-labeled RNAs were generated in vitro using RiboMAX™ Large Scale RNA Production System (Promega) and RNA 3' End Desthiobiotinylation Kit (Thermo Fisher) according to the manufacturer's instructions. The RNA-protein complexes were captured using Pierce™ Magnetic RNA-Protein Pull-Down Kit according to the manual (Thermo Fisher). The products were detected by Q-Exactive LC-MS (Thermo Fisher).

RNA fluorescence in situ hybridization (RNA-FISH) assay

RNA-FISH assay was performed as previously reported [32]. Biotin-TEG labeled seRNA-NPCm probes were purchased from Sangon Biotech Co. (Shanghai, China). The seRNA-NPCm was detected using Ribo™ Fluorescent In Situ Hybridization Kit (RiboBio, China) and Cy3-Streptavidin (K1079, APExBIO), according to the manual.

Transwell and wound healing assays

These assays were performed as previously reported [33]. In brief, cell migration and invasion analysis were detected using Transwell chambers according to the manufacturer's instructions (Corning Costar, 3422). For wound healing assay, we used a pipette tip to make a scratch wound. The cell numbers and percentage of healed area were measured by ImageJ software (NIH Image). For each of these assays, three independent experiments were performed.

RNA-seq and data analysis

RNA-seq assays were performed as previously reported [31]. In brief, total RNA was extracted from S26 cells and S26 cells treated with 120 μM DNP for 2 days. Samples with three biological replicates were sequenced at the Epibiotek Laboratory (Guangzhou Epibiotek Co., China) using the Illumina HiSeq2000 platform. Pair-

end raw reads were mapped to the human reference genome (GRch38) using Hisat2. Different gene analysis was performed using the DESeq2 algorithm. The criteria for statistical significance were $\log_2$FC > 1 and FDR < 0.05.

ChIP assay

ChIP assays were performed following previous protocol [29]. qPCR primers for target genomic locus are listed in Supplementary Data 3. The percentage of the input recovery was calculated.

ChIRP assay

ChIRP assays were performed following previous protocol [34]. The antisense oligos of seRNA-NPCm and qPCR primers are listed in Supplementary Data 3. The percentage of the input recovery was calculated.

GRO-seq

GRO-seq assays were performed as previously reported [29]. In brief, nuclear run-on buffer (NRO) and 5-bromouridine-5'-triphosphate (BrUTP) were used to generate BrU-tagged NRO RNAs, which were then reverse transcribed into cDNAs. The final cDNA libraries were sequenced using the Illumina HiSeq2500 platform.

DRIP assay

DRIP assays were performed as previously described [35]. qPCR primers for target genomic locus are listed in Supplementary Data 3. The percentage of the input recovery was calculated.

Single cell RNA-seq assay

Single cell RNA-seq assays were performed as previously reported [35]. We used the Cell Ranger software (10× Genomics) to filter, align, and quantify the raw data, and finally obtain the gene expression matrix of each cell. Seurat was applied for data normalization, clustering, T-distributed stochastic neighbor embedding (tSNE), and marker genes analysis in different clusters.

IHC and ISH assay

IHC assay and ISH assay were performed as previously described [36]. NPC tissue microarrays were purchased from Super Biotech Corporation (Shanghai, China). The microarray contains 126 NPC tissue and 14 para-carcinoma tissue. For ISH assay, the seRNA-NPCm probes were designed and synthesized by the Boster Corporation (China).

Data visualization

The data of ChIP-seq, GRO-seq, ChIRP-seq and DRIP-seq were visualized using IGV software. The GRO-seq data were visualized using UCSC genome browser. All heat maps and read density plots were drew using NGSPlot and R packages.

Statistical analysis

The statistical analyses were performed using Student's t test or ANOVA test. At least three biological replicates were performed for in vitro experiments, and a sample size of at least three to five mice was selected for in vivo experiments. Pearson's correlation coefficient assay was applied to analyze the relationship between seRNA-NPCm and NDRG1. The progression-free survival was analyzed using the log-rank test and Cox regression models. The intensity of Western blot band was quantified using ImageJ software. The difference was statistically significant when the *P*-value was less than 0.05.

Results

DNP induces the production of seRNA-NPCm in NPC cells

S26 and DNP-treated S26 (S26-DNP) cells were used to identify SEs through H3K27ac ChIP-seq. A total of 486 specific SEs were generated after DNP treatment (**Figure 1A**). Further global run-on sequencing (GRO-seq) analysis revealed that one of these special SE generated a novel seRNA named as seRNA-NPCm (**Figure 1B**). Rapid amplification of complementary DNA ends (RACE) analysis revealed seRNA-NPCm was a 3496 nt non-coding RNA (the sequence of seRNA-NPCm is listed in Supplementary Data 1). In S26 and S26-DNP cells, seRNA-NPCm was mainly localized in the nucleus (**Figure 1D**, **1E**), and cellular fractionation assay further verified it (**Figure 1F**). This suggests that seRNA-NPCm may function pri-

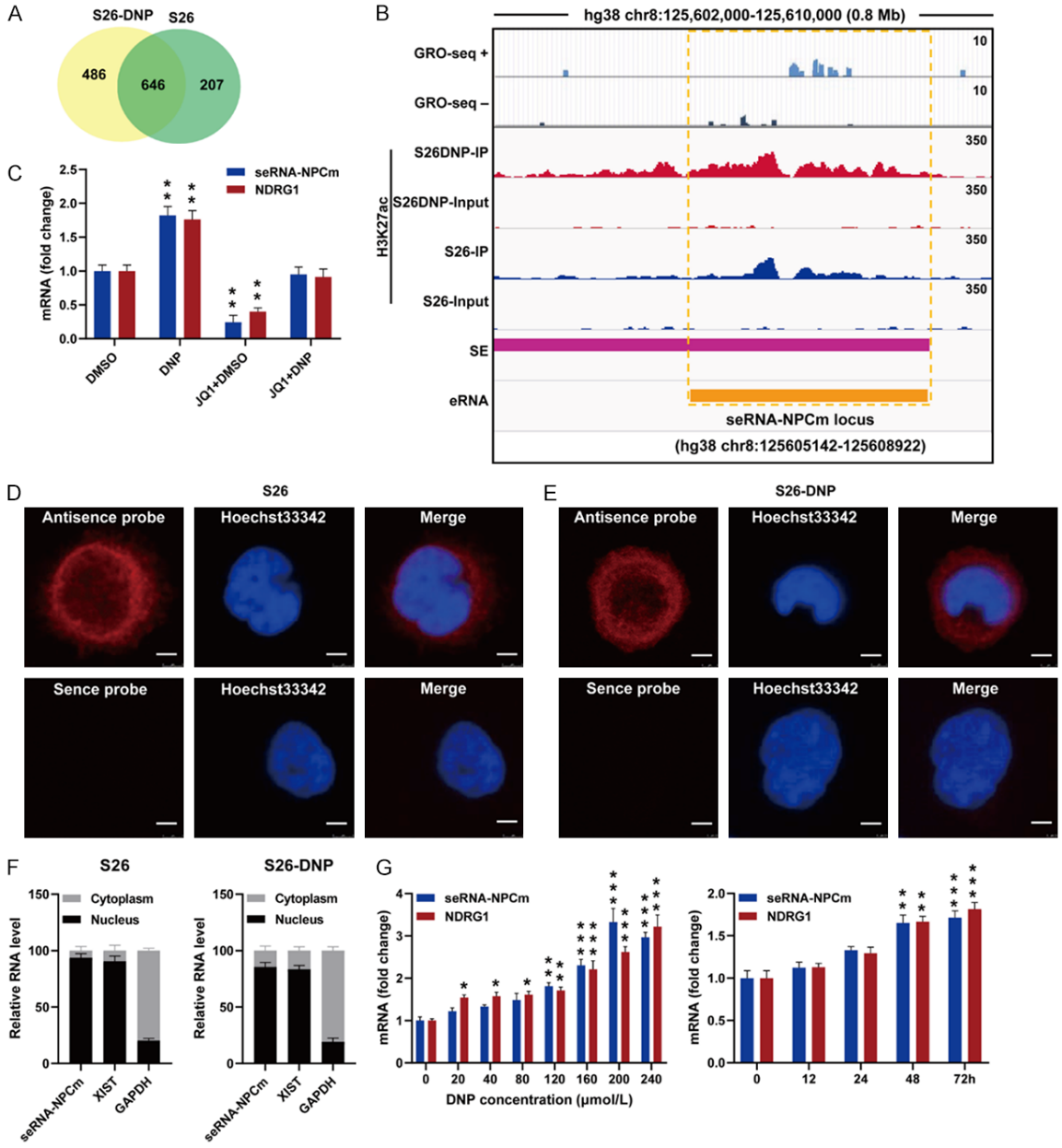

Figure 1. DNP induces the production of seRNA-NPCm in NPC cells. A. Venn diagrams of SEs in S26-DNP (yellow) and S26 (green). B. ChIP-seq for H3K27ac and GRO-seq (S26-DNP) signals at seRNA-NPCm locus. S26-DNP cells served as S26 cells treated with 120 μM DNP for 2d. C. The expression of seRNA-NPCm and NDRG1 mRNA in S26 cells treated with DMSO, DMSO+JQ1, DNP, and DNP+JQ1 (n = 3-5 independent experiments). Data are expressed as mean ± SEM; $^{**}P < 0.01$. D, E. Confocal fluorescence in situ hybridization images showing the localization of seRNA-NPCm in S26 and S26-DNP cells respectively using an antisense probe (red), with nuclei staining with Hoechst33342 (blue). Sense probe was used as negative control. Scale bars: 5 μm. F. qPCR analysis of RNAs purified from nuclear and cytosolic fractions of S26 and S26-DNP cells (n = 3-5 independent experiments). XIST and GAPDH are nuclear or cytoplasmic control, respectively. G. The expression dynamics of seRNA-NPCm and NDRG1 in various concentrations of DNP (n = 3-5 independent experiments). Data are expressed as mean ± SEM; $^{*}P < 0.05$, $^{**}P < 0.01$, $^{***}P < 0.001$.

marily in the nucleus. We next examined the expression dynamics of seRNA-NPCm in various concentrations of DNP. As shown in **Figure 1G**, seRNA-NPCm expression was evidently increased when the S26 cells were treated with 120 μM DNP for 2 days.

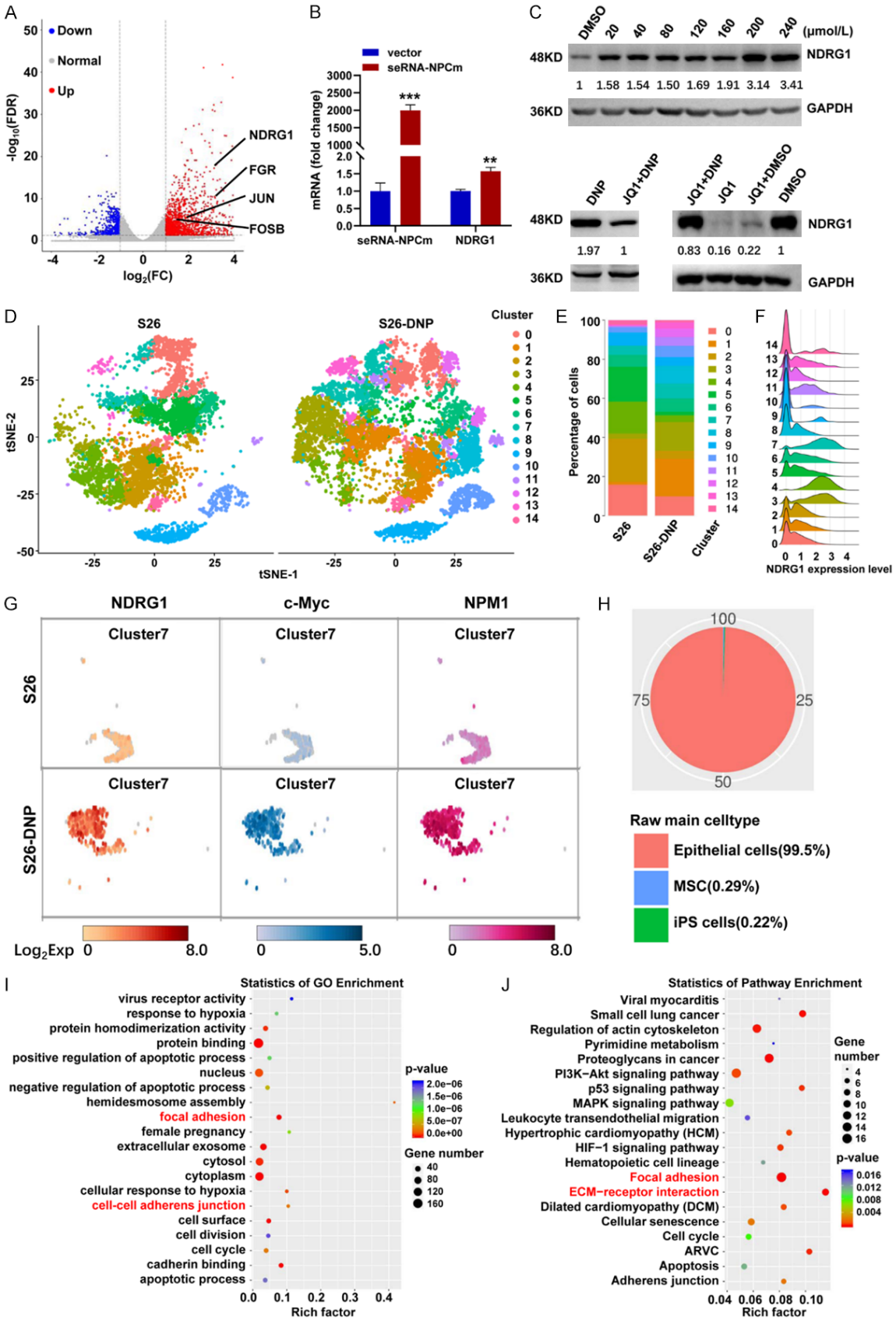
A
Down
Normal
Up
NDRG1
FGR
JUN
FOSB
-log10(FDR)
log2(FC)
B
vector
seRNA-NPCm
mRNA (fold change)
seRNA-NPCm
NDRG1
C
DMSO
20
40
80
120
160
200
240
(μmol/L)
48KD
NDRG1
1 1.58 1.54 1.50 1.69 1.91 3.14 3.41
36KD
GAPDH
DNP
JQ1+DNP
JQ1+DNP
JQ1
JQ1+DMSO
DMSO
1.97 1
0.83 0.16 0.22 1
D
S26
S26-DNP
Cluster
tSNE-1
tSNE-2
E
Percentage of cells
S26
S26-DNP
Cluster
F
NDRG1 expression level
G
NDRG1
c-Myc
NPM1
Cluster7
S26
S26-DNP
Log2Exp
H
Raw main celltype
Epithelial cells(99.5%)
MSC(0.29%)
iPS cells(0.22%)
I
Statistics of GO Enrichment
virus receptor activity
response to hypoxia
protein homodimerization activity
protein binding
positive regulation of apoptotic process
nucleus
negative regulation of apoptotic process
hemidesmosome assembly
focal adhesion
female pregnancy
extracellular exosome
cytosol
cytoplasm
cellular response to hypoxia
cell-cell adherens junction
cell surface
cell division
cell cycle
cadherin binding
apoptotic process
Rich factor
p-value
Gene number
J
Statistics of Pathway Enrichment
Viral myocarditis
Small cell lung cancer
Regulation of actin cytoskeleton
Pyrimidine metabolism
Proteoglycans in cancer
PI3K−Akt signaling pathway
p53 signaling pathway
MAPK signaling pathway
Leukocyte transendothelial migration
Hypertrophic cardiomyopathy (HCM)
HIF−1 signaling pathway
Hematopoietic cell lineage
Focal adhesion
ECM−receptor interaction
Dilated cardiomyopathy (DCM)
Cellular senescence
Cell cycle
ARVC
Apoptosis
Adherens junction
Rich factor
Gene number
p-value

Figure 2. DNP-induced seRNA-NPCm promotes NDRG1 transcription. A. The volcano plots of RNA-seq data (S26-DNP vs. S26), FC represents fold change, FDR represents false discovery rate. B. qPCR analysis of the seRNA-NPCm and NDRG1 transcript levels in 6-10B cells transfected with vector or seRNA-NPCm (n = 3-5 independent experiments). Data are expressed as mean ± SEM; $^{**}P < 0.01$, $^{***}P < 0.001$. C. Top shows the expression dynamics of NDRG1 protein in various concentrations of DNP. Bottom shows the expression of NDRG1 protein in S26 cells treated with DNP, JQ1+DNP, JQ1, JQ1+DMSO, and DMSO. D. The tSNE diagram of the cluster of single-cell subsets. Different colors indicate different clusters. E. The proportion of each cluster cells in S26 and S26-DNP groups. F. Ridge plot of NDRG1 gene in different clusters. NDRG1 is highly expressed in cluster 3, 4, and 7. G. The expression levels of NDRG1, c-Myc, and NPM1 in cluster 7 of S26 and S26-DNP. H. The cell-types identified in cluster 7 and their percentages. I, J. Scatter plot of GO and KEGG enrichment of differentially expressed genes in cluster 7. Rich factor represents the number of differential genes located in the GO or KEGG/the total number of genes located in the GO or KEGG. ARVC: Arrhythmogenic right ventricular cardiomyopathy.

BRD4 (bromodomain-containing protein 4) is an important coactivator that can assemble different transcriptional complexes on the SE and recruit RNAP II for transcription initiation [37]. JQ1 can inhibit seRNAs transcription through preventing BRD4 from connecting with H3K27ac at SEs [38]. NPC cells were treated with JQ1 or DNP+JQ1 for 48 h and the seRNA-NPCm expression was tested by qRT-PCR. The results showed that JQ1 blocked the function of DNP in inducing seRNA-NPCm production (**Figure 1C**, $P < 0.01$). These results reveal that DNP has the capacity to induce the generation of seRNA-NPCm.

DNP-induced seRNA-NPCm promotes NDRG1 transcription

eRNAs have been shown to activate the transcription of target genes [29, 32]. DNP-induced seRNA-NPCm may involve in oncogene expression. RNA-seq analysis showed that DNP treatment led to significant increases in the expression of several oncogenes, including *NDRG1*, *JUN*, *FOSB*, *FGR*, etc. ($\log_2$FC > 1, FDR < 0.05) (**Figure 2A**). qPCR detection showed NDRG1 upregulation at mRNA when transfected with seRNA-NPCm (**Figure 2B**), and Western blot assay revealed that NDRG1 expression was upregulated by DNP (**Figure 2C** up panel), while NDRG1 expressions decreased in JQ1 plus DNP and JQ1 plus DMSO respectively compared with DNP and DMSO controls (**Figure 2C** down panel). These results revealed that DNP-induced seRNA-NPCm might upregulate target gene NDRG1.

To further explore the role of DNP in NPC metastasis, DNP-induced metastases were examined using single-cell RNA sequencing. S26 and S26-DNP cells were injected into the tail vein of nude mice. After 30 days, subcutaneous metastases were collected for single-cell RNA sequencing. All these cells were divided into virous clusters by a clustering algorithm based on the shared nearest neighbor (SNN) (**Figure 2D**). Further analysis revealed that one of the clusters with high NDRG1 expression was abundant in S26-DNP compared to S26 (**Figure 2E-G**). In addition, the mRNA levels of c-Myc and NPM1 were elevated in this cluster of S26-DNP metastasis (**Figure 2G**). Gene Ontology (GO) and Kyoto Encyclopedia of Genes and Genomes (KEGG) analyses showed this cluster was mainly involved in cell-cell adhesion junction, focal adhesion and extracellular matrix (ECM)-receptor interaction (**Figure 2I**, **2J**), suggesting that it might be essential for the regulation of cellular proliferation, adhesion, and migration. Then we used the reference data set provided by SingleR to identify this cluster. The results showed that part of this cluster cells presented iPSC-like characteristics (**Figure 2H**). All these results suggest that the ability of DNP to promote NPC metastasis may be related to regulation of NDRG1 expression.

seRNA-NPCm regulates NDRG1 through binding with NPM1/MYC

To investigate the molecular mechanism by which seRNA-NPCm regulates NDRG1 transcription, we applied RNA pull-down assay to identify protein partners of seRNA-NPCm. Mass spectrometry (MS) analysis of coprecipitated products showed that NPM1 was one of the top 7 seRNA-NPCm interacting TFs (**Figure 3D**), Public data reveal that c-Myc protein can bind to the promoter of NDRG1 (**Figure 3A**). This interaction was further confirmed by Western blot (**Figure 3B**). To further study the binding properties, truncated fragments of seRNA-NPCm were used to specify the NPM1 interact-

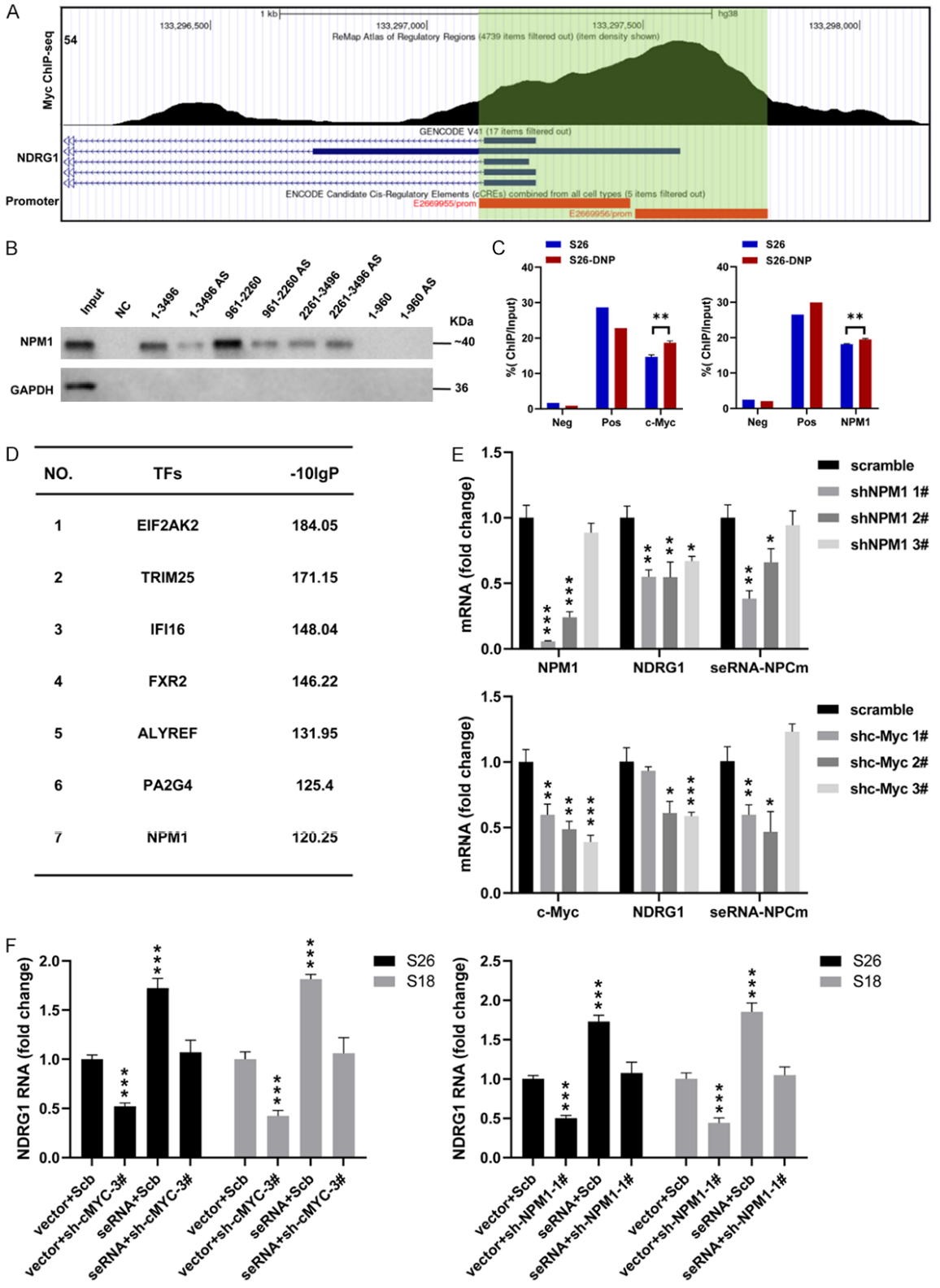

Figure 3. seRNA-NPCm regulates NDRG1 through binding with NPM1/MYC. A. c-Myc ChIP-seq signals at promoter of NDRG1. The data was downloaded from UCSC. B. The indicated deletion fragments of seRNA-NPCm and its interacting region with NPM1. AS stands for antisense. GAPDH was negative control. C. qPCR verified NPM1 and c-Myc enrichment at NDRG1 promoter. For c-Myc ChIP-qPCR, alpha-Satellite and NPM1 were negative and positive control, respectively. For NPM1 ChIP-qPCR, FBP1-NEG and FBP1-POS were negative and positive control, respectively; $^{**}P < 0.01$. D. The top 7 interacting TFs of seRNA-NPCm from RNA pull down-MS results. E. The transcript levels in S26

cells stably transfected with shRNAs targeting NPM1, c-Myc or scrambled negative control. F. qPCR indicating the NDRG1 levels in NPC cells stably transfected with vector or seRNA, and those co-transfected with sh-cMYC-3# or sh-NPM1-1#. The expression of target genes was measured by qPCR (n = 3 independent experiments). Data are expressed as mean ± SEM; *$P < 0.05$, **$P < 0.01$, ***$P < 0.001$.

ing regions. The results that showed a 1300 nt region in the middle of seRNA-NPCm (961-2260 nt) was essential for interaction with NPM1 (**Figure 3B**). NPM1 is a cofactor for *c-Myc* activity. It interacts with c-Myc and the NPM1/c-Myc complex binds to the promoter of *c-Myc* target genes to regulate their transcription [39]. ChIP-qPCR analysis further verified that c-Myc enrichment level at promoter of NDRG1 in S26-DNP cells was higher than that in S26 cells (**Figure 3C**). In addition, NPM1 enrichment was also higher at NDRG1 promoter in S26-DNP cells (**Figure 3C**). Knockdown of either NPM1 or c-Myc resulted in a significant decrease in NDRG1 (**Figure 3E**). Further rescue assays showed that overexpression of seRNA-NPCm restored NDRG1 expression that was reduced by knockdown of NPM1 or c-MYC (**Figure 3F**).

seRNA-NPCm promotes chromosome looping by forming R-loop at SE region

To confirm DNA binding sites of seRNA-NPCm, chromatin isolation by RNA purification and sequencing (ChIRP-seq) analysis was conducted to investigate DNP-mediated molecule mechanism. Overexpressed-seRNA-NPCm S26 cells were used in ChIRP test because seRNA-NPCm expression in NPC cells was very low. The results showed a strong specific signal in the SE region 41.8 Kb upstream of NDRG1 (**Figure 4A**). Further qPCR test confirmed it (**Figure 4B**). The above results indicate that seRNA-NPCm can bind in this SE region. The deletion of this SE using CRISPR Cas9 (**Figure 4C**) led to decreased expression of NDRG1 (**Figure 4D**), indicating that this SE region plays an important role in NDRG1 expression. Analysis of public data from DNase-seq, ATAC-seq, and CTCF ChIP-seq showed that the seRNA-NPCm binding region was near with CTCF and chromatin accessibility, suggesting that seRNA-NPCm may be involved in chromatin looping (**Figure 4E**).

MeDIP-seq data showed that the seRNA-NPCm binding region upstream of NDRG1 is hypomethylated in both K562 and GM12878 cells (**Figure 4F**). Considering that R-loops are often formed in hypomethylated regions [40, 41], it is possible that seRNA-NPCm binds to the SE region to form an R-loop structure. To this end, DNA-RNA immunoprecipitation (DRIP) assay was performed to recognize DNA-RNA hybrids (R-loop). The results showed that the SE region upstream of NDRG1 presented a distinct DRIP-seq signal (**Figure 4G**). Further qPCR detection showed that overexpressed-seRNA-NPCm S26 cells had an increased enrichment of the R-loop in this SE region compared to S26 cells (**Figure 4H**), suggesting that seRNA-NPCm might form an R-loop in this SE region. To clarify the properties of seRNA-NPCm forming the R-loop, we performed DRIP-qPCR assays using cells stably overexpressing the truncated seRNA-NPCm fragments. The results showed that the deletion of 1236 nt region at the 3' end (2261-3496 nt) of seRNA-NPCm prevented the formation of R-loop in this SE region (**Figure 4H**), suggesting that it might be the DNA binding domain of seRNA-NPCm. These results suggest that the 3' end (2261-3496 nt) of seRNA-NPCm may hybridize to SE to form an R-loop. Meanwhile, the above results show that the middle region of seRNA-NPCm binds to the NPM1/c-Myc complex and anchors to the NDRG1 promoter. seRNA-NPCm may act as a lasso to facilitate chromatin looping and interactions between SE and promoter, resulting in the upregulation of NDRG1 (**Figure 4I**).

DNP-induced seRNA-NPCm promotes NPC metastasis in vitro

To explore the effect of DNP-induced seRNA-NPCm on NPC metastasis in vitro, S26 and 6-10B are NPC cell lines with low metastatic ability, S26 treated with DMSO, DMSO plus JQ1, DNP, or DNP+JQ1, and 6-10B cells treated with DMSO, DMSO plus JQ1, DNP, or DNP+JQ1 were used for wound healing assay, Transwell assay (migration assay), matrigel Transwell assay (invasion assay), respectively. These assays showed that DNP treatment increased the migration and invasion capacities of S26 and 6-10B cells, which were blocked by JQ1 (**Figure 5A-C**, $P < 0.001$), indicating that DNP promoted NPC migration and invasion by pro-

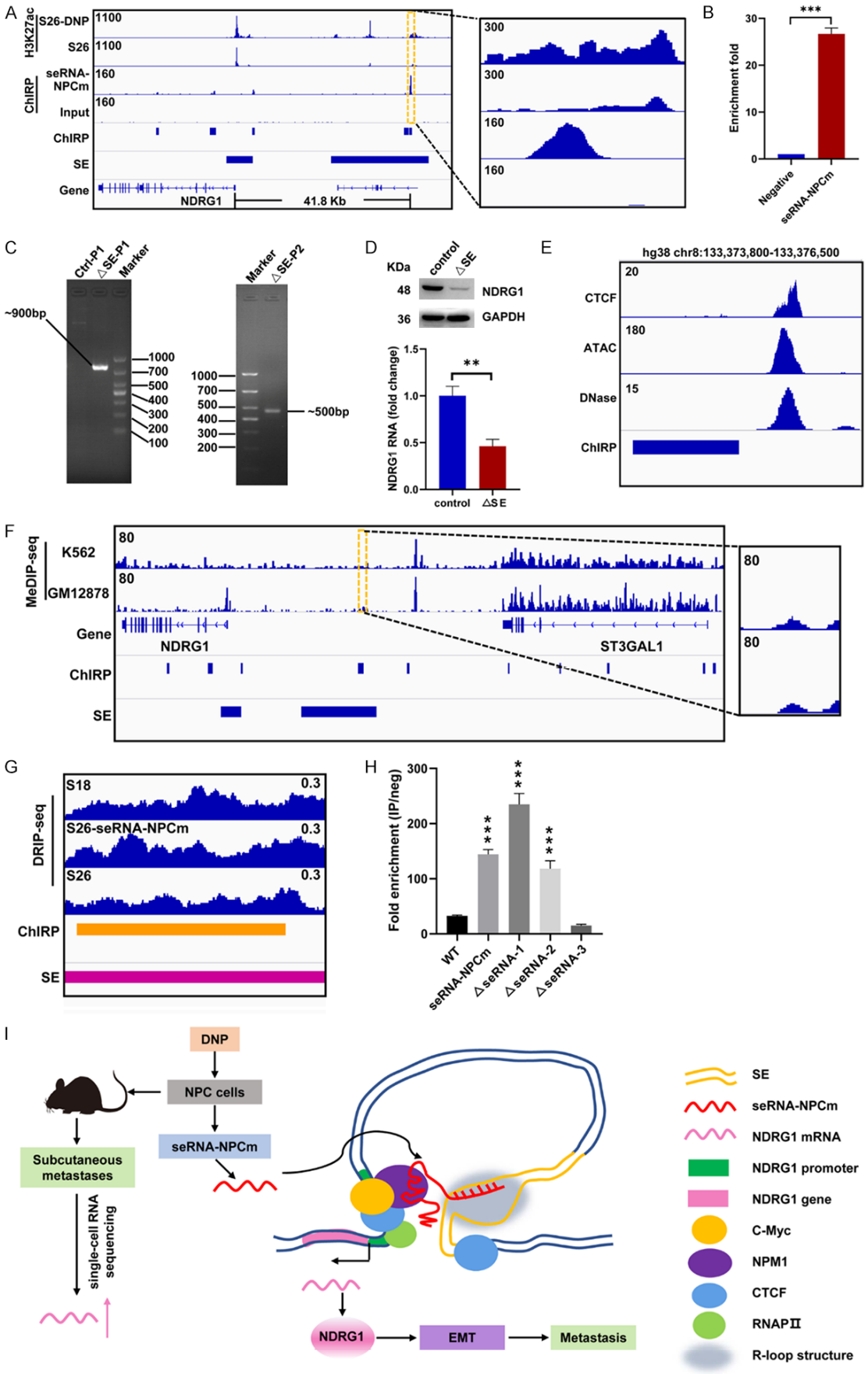
A
H3K27ac
S26-DNP
S26
ChIRP
seRNA-NPCm
Input
ChIRP
SE
Gene
NDRG1
41.8 Kb
B
Enrichment fold
Negative
seRNA-NPCm
C
Ctrl-P1
△SE-P1
Marker
~900bp
~500bp
D
KDa
control
△SE
NDRG1
GAPDH
NDRG1 RNA (fold change)
E
hg38 chr8:133,373,800-133,376,500
CTCF
ATAC
DNase
ChIRP
F
MeDIP-seq
K562
GM12878
Gene
NDRG1
ST3GAL1
ChIRP
SE
G
DRIP-seq
S18
S26-seRNA-NPCm
S26
ChIRP
SE
H
Fold enrichment (IP/neg)
WT
seRNA-NPCm
△seRNA-1
△seRNA-2
△seRNA-3
I
DNP
NPC cells
seRNA-NPCm
Subcutaneous metastases
single-cell RNA sequencing
NDRG1
EMT
Metastasis
SE
seRNA-NPCm
NDRG1 mRNA
NDRG1 promoter
NDRG1 gene
C-Myc
NPM1
CTCF
RNAPII
R-loop structure

Figure 4. seRNA-NPCm promotes chromosome looping by forming R-loop at SE region. A. SeRNA-NPCm ChIRP-seq signals at the SE 41.8 Kb upstream of NDRG1 promoter. B. qPCR verified seRNA-NPCm enrichment at the SE 41.8 Kb upstream of NDRG1 promoter. C. The seRNA-NPCm binding region inside the SE upstream of NDRG1 promoter was deleted using CRISPR interference, the nested PCR was used to verify the knockout efficiency. D. NDRG1 mRNA and protein expression in ΔE S26 cells and control cells. ΔE, S26 cells with seRNA-NPCm binding SE deletion. (n = 3-5 independent experiments). Data are expressed as mean ± SEM; $^{**}P < 0.01$. E. ATAC-seq (HepG2, GSE170012), DNase-seq (Hela-S3, GSE90432), and CTCF ChIP-seq (HepG2, GSE170879) signals at seRNA-NPCm binding site. F. MeDIP-seq signals in seRNA-NPCm binding DNA site. MeDIP-seq data were downloaded from ENCODE database, K562 (GSM1368906) and GM12878 (GSM1368907). G. DRIP-seq detected the R-loop signals at the seRNA-NPCm binding site in S26, S18, and overexpressed-seRNA-NPCm S26 cells. H. The R-loop signals at the seRNA-NPCm binding site in S26 cells expressing different fragments of seRNA-NPCm. ΔseRNA-1 represents the deletion of 1-960 nt of seRNA-NPCm, ΔseRNA-2 represents the deletion of 961-2260 nt of seRNA-NPCm, ΔseRNA-3 represents the deletion of 2261-3496 nt of seRNA-NPCm. Data are expressed as mean ± SEM; $^{***}P < 0.001$. I. The model of DNP-induced seRNA-NPCm facilitating NPC metastasis through regulation of NDRG1 expression.

ducing seRNAs. S18 and 5-8F are high metastatic cell lines, they were used to test the effect of sh-seRNA-NPCm on NPC cell metastases. Downregulation of seRNA-NPCm reduced the migration and invasion of S18 and 5-8F cells (**Figure 5D**, $P < 0.001$), suggesting that seRNA-NPCm might be an important macromolecular in regulating the cell motility of NPC.

DNP-induced seRNA-NPCm promotes NPC metastasis in vivo

We further evaluated the effect of DNP-induced seRNA-NPCm on NPC metastasis in vivo. Luciferase-labeled S26, S26-DNP, and highly metastatic NPC cell S18 were injected into the tail vein of nude mice. The nude mice were female BALB/c nude mice at 4-6 weeks, 6 mice/group. Their abilities to form pulmonary metastasis were examined 30 days later. The results showed that nude mice injected with S26-DNP and S18 cells presented larger metastatic lesions than those injected with S26 cells (**Figure 6A**). Immunohistochemistry (IHC) was used to detect EMT markers including E-cad, N-cad, Vimentin, and Snail in the metastatic tumor tissues, IHC staining were quantified and were statistically analyzed. IHC staining of pulmonary metastases and quantitative analysis showed that E-cadherin was decreased, N-cadherin, Snail, and Vimentin were elevated in S26-DNP and S18 group (**Figure 6B**, $P < 0.01$ or 0.001). Further analysis showed that nude mice given injections of overexpressed-seRNA-NPCm S26 cells had decreased survival, loss of body weight (**Figure 6C**). Overexpressed-seRNA-NPCm S26 cells formed more metastases at 1 weeks after injection (**Figure 6D**, **6E**). IHC staining of pulmonary metastases showed that E-cadherin was decreased, N-cadherin, Snail, and vimentin were elevated in seRNA-NPCm group (**Figure 6F**, **6G**). Altogether, these findings revealed that DNP-induced seRNA-NPCm promotes NPC metastasis. Continued bioluminescence imaging (BLI) showed the recovery of NDRG1 in overexpressed-seRNA-NPCm S26 cells restored the ability of S26 to form lung metastases (**Figure 6D**), indicating a role of NDRG1 in seRNA-NPCm--mediated metastasis formation of NPC cells. Further in vitro assays also revealed that knockdown of NDRG1 suppressed NPC cell motility (**Figure 6H**, $P < 0.001$).

NDRG1 is a poor prognostic indicator for NPC patients

The expression levels of seRNA-NPCm and NDRG1 in a tissue microarray containing 126 NPC patients were detected by RNA in situ hybridization (ISH) and IHC staining. In comparison to para-carcinoma tissue, NPC tissues presented higher expression levels of NDRG1 and seRNA-NPCm, especially in advanced NPC samples (**Figure 7A**, **7B**). NPC patients with highl seRNA-NPCm ($P < 0.05$) and NDRG1 expressions ($P < 0.05$) presented shorter progression-free survival times (**Figure 7C**). Furthermore, there is a positive correlation between seRNA-NPCm and NDRG1 expression in NPC tissues (R, 0.501, $P < 0.05$) (**Figure 7D**). Multivariate Cox regression analysis showed that the independent prognostic factors included TNM stage ($P < 0.05$), and the expression of NDRG1 protein ($P < 0.05$) (Supplementary Data 2). These findings indicate that NDRG1 is an indicator of poor prognosis for NPC patients.

Discussion

DNP has been shown to be closely related to the oncogenesis and development of NPC.

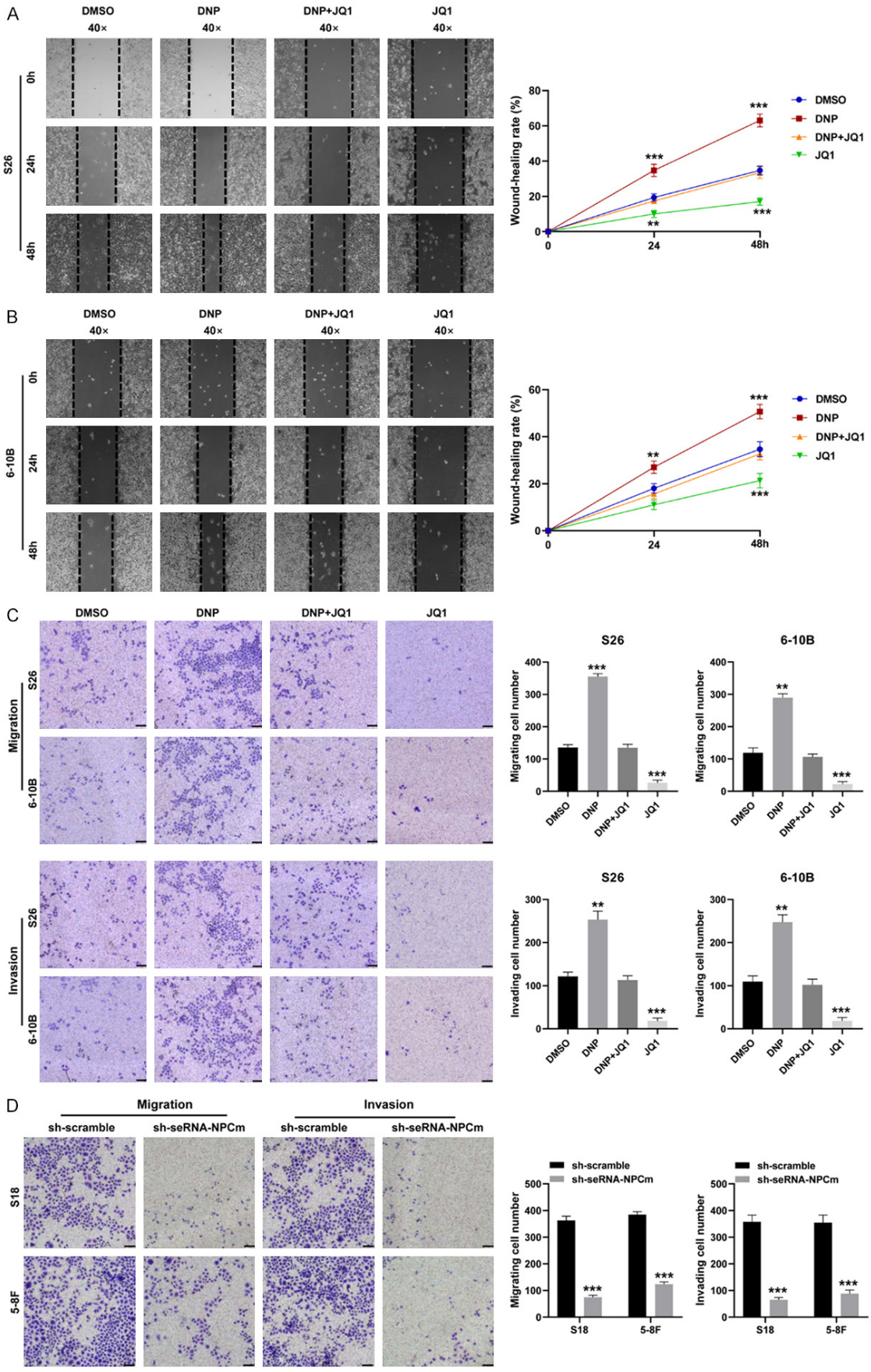
A
DMSO
DNP
DNP+JQ1
JQ1
40×
S26
0h
24h
48h
Wound-healing rate (%)
DMSO
DNP
DNP+JQ1
JQ1
B
6-10B
C
Migration
Invasion
S26
6-10B
Migrating cell number
Invading cell number
D
Migration
Invasion
sh-scramble
sh-seRNA-NPCm
S18
5-8F

Figure 5. DNP-induced seRNA-NPCm promotes NPC metastasis in vitro. A, B. Migration of S26 and 6-10B cells treated with DMSO, DNP, DNP+JQ1, and JQ1 (n = 3 independent experiments). C. Migration and invasion of S26 and 6-10B cells treated with DMSO, DNP, DNP+JQ1, and JQ1 (n = 3 independent experiments). Scale bars, 200 μm. D. Migration and invasion of S18 and 5-8F cells transfected with shseRNA-NPCm or shscramble (n = 3 independent experiments). Scale bars, 200 μm. Data are expressed as mean ± SEM; $^{**}P < 0.01$, $^{***}P < 0.001$.

However, the mechanism of DNP carcinogenesis remains unclear. In this work, we demonstrated that elevated seRNA-NPCm induced by DNP resulted in upregulation of NDRG1, as well as increased metastatic capacity and iPSC-like properties of NPC cells. Assays by restoring NDRG1 expression showed reversed metastatic capacity. Further studies show that seRNA-NPCm acts as a lasso to pull SE and promoter close to each other by binding to NPM1/c-Myc complex and forming an R-loop structure in SE region, resulting in NDRG1 transcription. Our study reveals that seRNA-NPCm-mediated NDRG1 upregulation plays an important role in DNP-induced NPC metastasis.

An increasing number of non-coding RNAs (ncRNAs) have been shown to participate in the oncogenesis and development of tumors. eRNAs are ncRNAs that partly function to promote enhancer-promoter looping and mRNA transcription [31, 42, 43]. For instance, heparanase (HPSE) eRNA interacts with hnRNPU/p300/EGR1 to loop chromatin between SE and HPSE promoter, thereby activating HPSE expression to promote tumor progression in cancers [43]. Depletion of seRNA generated by SEs downstream of the MYC gene reduced MYC mRNA level in primary effusion lymphoma cells [29]. Besides binding to protein partners, eRNAs also interact with DNAs to modulate enhancer/SE function. Long noncoding RNA (lncRNA) auxin-regulated promoter loop (APOLO) recognizes target promoters and modulates transcription by the formation of R-loops [44], GATA3-AS1 lncRNA can form R-loops upstream of the GATA3 TSS to regulate the expression of GATA3 [45], suggesting R-loops play important roles in lncRNA-mediated transcriptional regulation. Increased seRNA hybridized with DNAs to form R-loop structure and resulted in genomic instability at SEs [15]. PEARL (protocadherin eRNA associated with R-loop formation) forms R-loops within the HS5-1 enhancer region to facilitate long-distance chromatin interactions between distal enhancers and promoters, resulting in protocadherin alpha gene expression [34]. In this paper, seRNA-NPCm was found to form R-loops in the SEs to promote chromatin interactions between SEs and promoters, resulting in target NDRG1 expression.

NPM1 is reported to participate in ribosome biogenesis, chromatin remodeling, cell proliferation, and tumorigenesis [46]. The structure of NPM1 protein mainly contains three regions: the conserved N-terminal domain that interactions with molecular chaperones and mediates oligomerization, the central acidic region for histone binding, and the C-terminal RNA-binding domain [47]. Previous study reveals that NPM1 co-localizes with c-Myc, c-Fos, P53 and Rb proteins [48]. NPM1 regulates the transcriptional activity of oncogenic c-Myc due to its ability to interact with c-Myc and be recruited to c-Myc target gene promoters [39]. NPM1 expression is necessary for induction of c-Myc target genes, however, the effect of NPM1 on c-Myc is not mediated by a significant increase in total NPM1 levels [49]. In addition, NPM1 might serve as a TF to regulate gene transcription. A recent study showed that NPM1 bound to programmed cell death ligand-1 (PD-L1) promoter in triple-negative breast cancer (TNBC) cells and facilitated PD-L1 transcription. Poly (ADP-ribose) polymerase 1 (PARP1) inhibited PD-L1 transcription through interaction with NPM1 [50]. NPM1 is also reported to bind to G-quadruplex forming regions, which are closely related to oncogene promoters, such as c-Myc, k-ras, bcl2, and so on [51]. The promoter of NDRG1 is shown to form G-quadruplexes, suggesting that NPM1 might bind to NDRG1 promoter to regulate its transcription. Our results further revealed that seRNA-NPCm bound to NPM1/c-Myc complex, which then anchored to the promoter of NDRG1, resulting in regulation of its transcription.

In this paper, we demonstrated that seRNA-NPCm regulates chromatin looping through forming R-loops in the SE region of NDRG1 to drive the metastatic transcription in NPC cells. However, NPC is a disease with diverse genetic and epigenetic alterations. Further investigation of the role of seRNA-NPCm--mediated

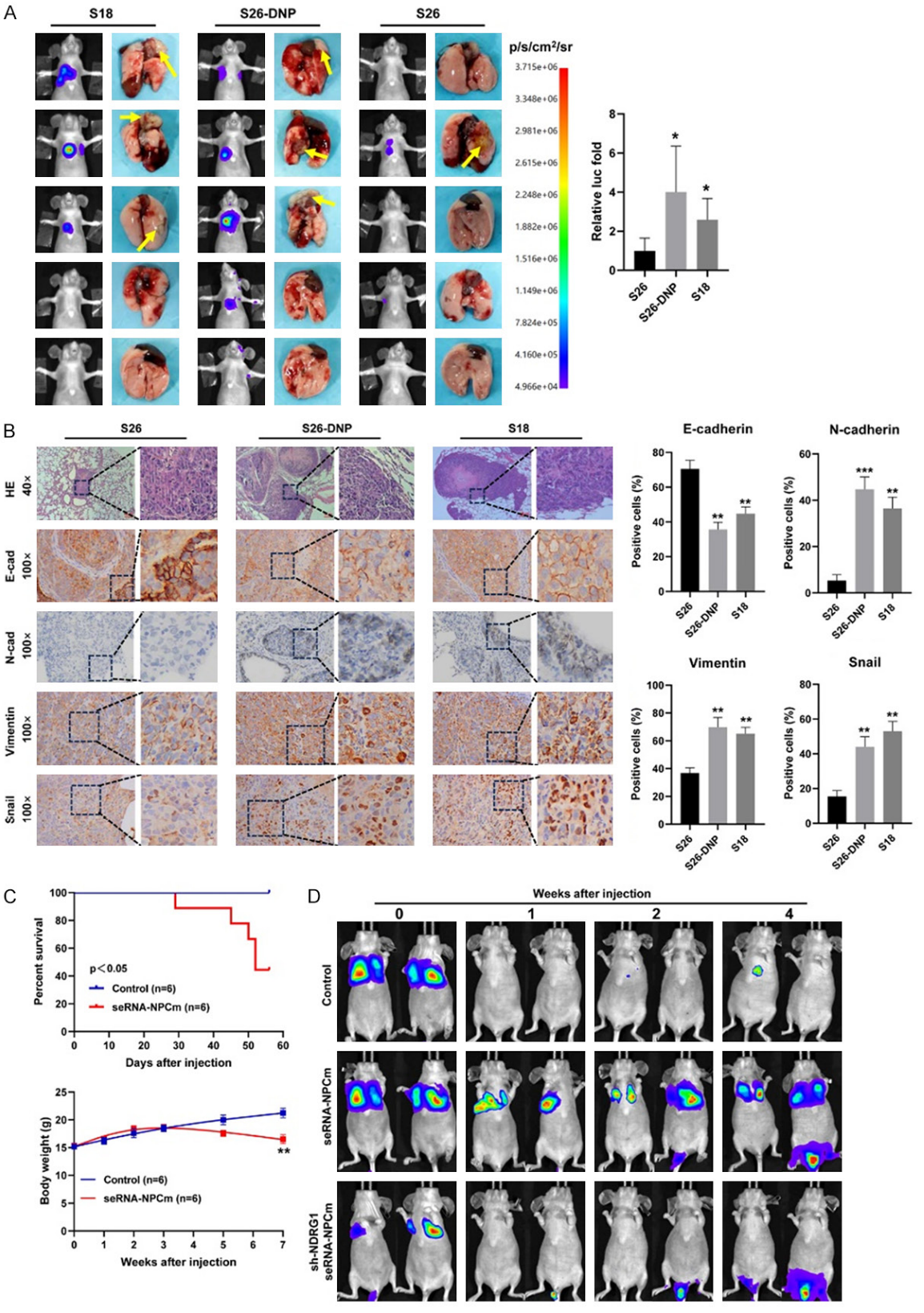
A
S18
S26-DNP
S26
p/s/cm²/sr
3.715e+06
3.348e+06
2.981e+06
2.615e+06
2.248e+06
1.882e+06
1.516e+06
1.149e+06
7.824e+05
4.160e+05
4.966e+04
Relative luc fold
S26
S26-DNP
S18
B
S26
S26-DNP
S18
HE 40×
E-cad 100×
N-cad 100×
Vimentin 100×
Snail 100×
E-cadherin
N-cadherin
Vimentin
Snail
Positive cells (%)
C
Percent survival
p<0.05
Control (n=6)
seRNA-NPCm (n=6)
Days after injection
Body weight (g)
Control (n=6)
seRNA-NPCm (n=6)
Weeks after injection
D
Weeks after injection
0
1
2
4
Control
seRNA-NPCm
sh-NDRG1 seRNA-NPCm

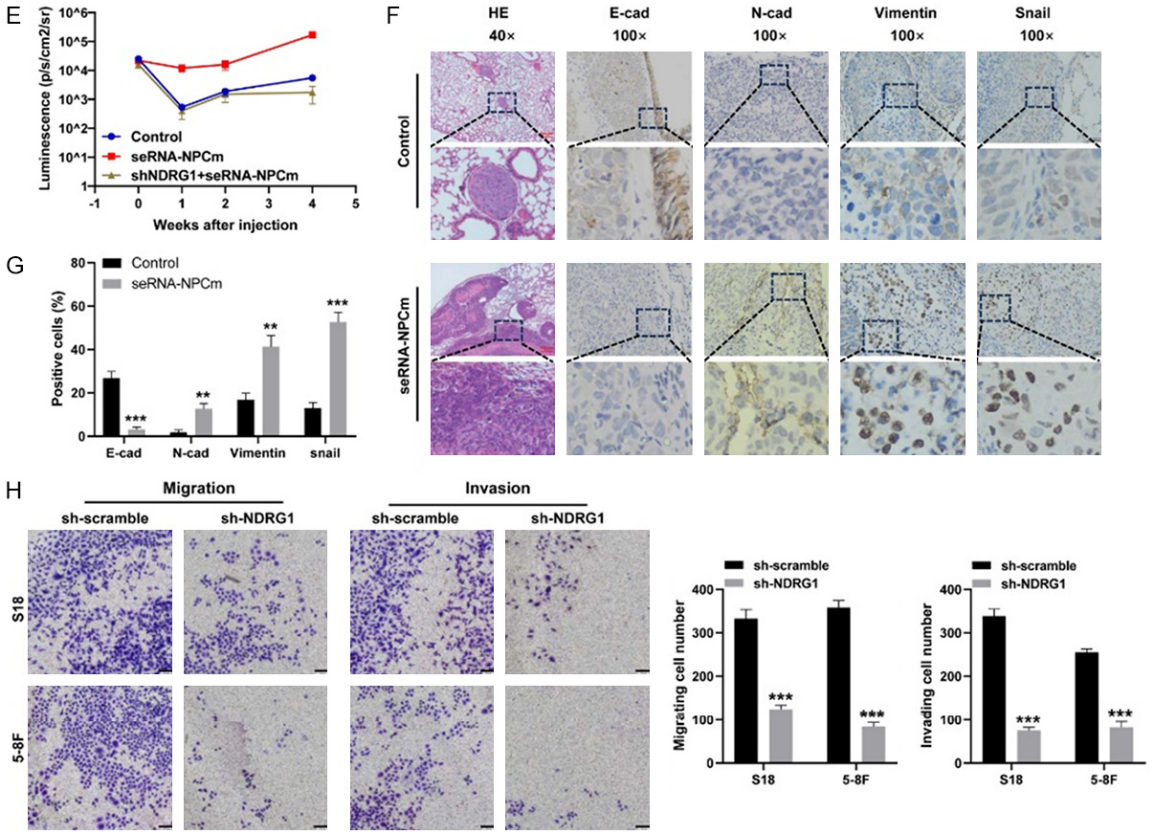

Figure 6. DNP-induced seRNA-NPCm promotes NPC metastasis in vivo. A. In vivo imaging of nude mice metastatic status by luciferase-based bioluminescence imaging. Yellow arrow, metastatic nodules; **P* < 0.05. B. IHC staining of E-cadherin, N-cadherin, Vimentin, and Snail in pulmonary metastases of indicated mice group. Scale bars, 100 μm. C. Top, Kaplan-Meier survival curve of mice; Bottom, the body weight of nude mice after tail vein injection of NPC cells. D, E. S26 cells transfected with the indicated lentivirus containing luciferase gene were injected in the tail vein of nude mice. BLI monitored the lung metastases formed from injected cells. Data are expressed as mean ± SEM. F, G. IHC staining of E-cadherin, N-cadherin, Vimentin, and Snail in pulmonary metastases of indicated mice group. Scale bars, 100 μm. H. Migration and invasion of S18 and 5-8F cells transfected with shNDRG1 or shscramble (n = 3 independent experiments). Scale bars, 200 μm. Data are expressed as mean ± SEM; ****P* < 0.001.

R-loops in the modulation of gene expression could further elucidate the relevance of this mechanism to NPC metastasis. seRNA-NPCm interacts with the NPM1/c-Myc complex and NPM1 contains an RNA-binding domain, whether other seRNAs mediate chromatin remodeling and gene transcription through NPM1/c-Myc remains unknown and requires further investigation.

Acknowledgements

The authors are grateful to all the investigators involved. This work was supported in part by the National Natural Science Foundation of China (81872226), Natural Science Foundation of Hunan Province (2018JJ6131, 2019JJ40175, and 2021JJ70098), Changsha Science and Technology Project (kg1801107 and kq2004-136), and Research Projects of Hunan Health Commission (B2019084), Major Scientific and Technological Innovation Project of Hunan Province (2021SK1020-4), China Postdoctoral Science Foundation (2022M711125).

Disclosure of conflict of interest

None.

Address correspondence to: Dr. Faqin Tang, Hunan Key Laboratory of Oncotarget Gene and Clinical Laboratory of Hunan Cancer Hospital, The Affiliated Cancer Hospital of Xiangya School of Medicine, Central South University, Changsha 410013, Hunan, China. Tel: +86-731-89762688; Fax: +86-731-89762688; E-mail: tangfq@hnca.org.cn

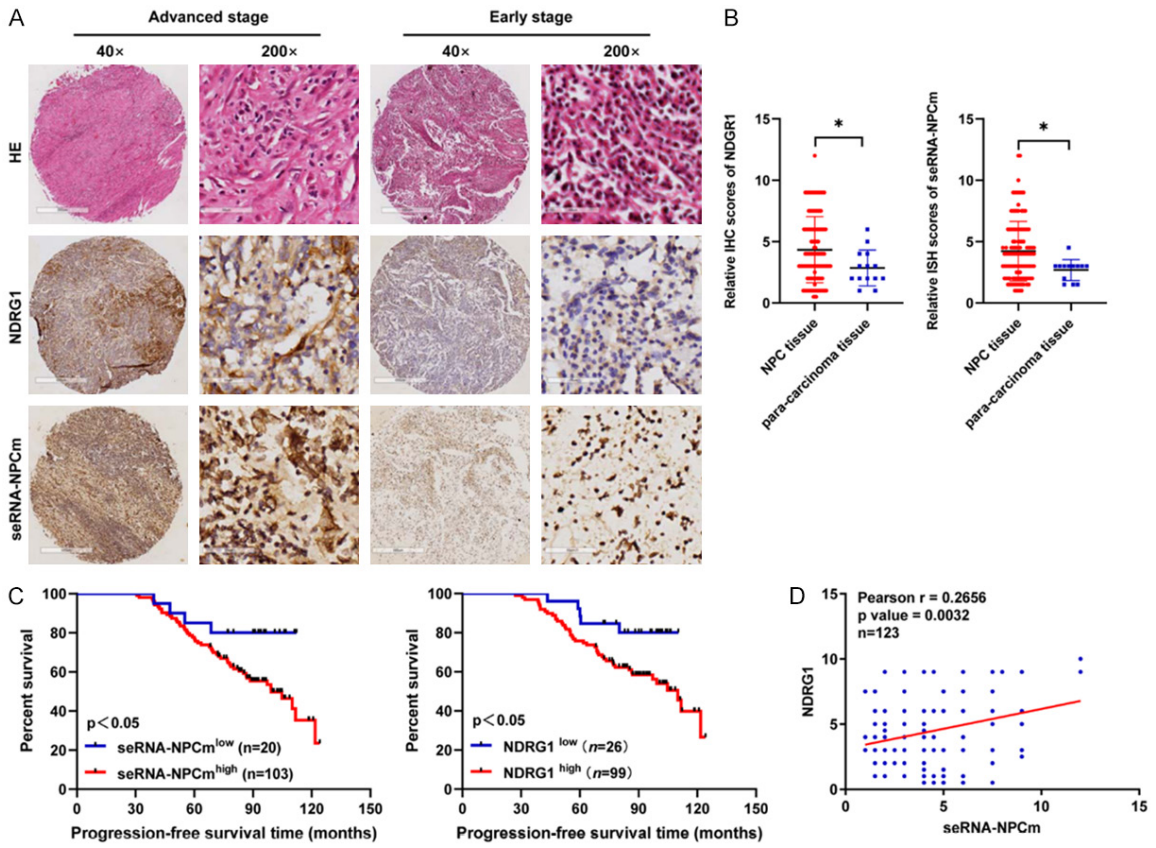

Figure 7. NDRG1 is a poor prognostic indicator for NPC patients. A. The expression of NDRG1 and seRNA-NPCm in NPC patients with different stages. HE staining results were downloaded from Super Biotech Corporation. B. The expression of seRNA-NPCm and NDRG1 in NPC patients. Para-carcinoma tissues were used to be control; **P* < 0.05. C. Kaplan-Meier survival curve of NPC patients with high (red) or low (blue) expression of seRNA-NPCm (left) and NDRG1 (right). D. Pearson's correlation analysis of seRNA-NPCm and NDRG. Data are expressed as mean ± SEM.

References

[1] Cho WC. Nasopharyngeal carcinoma: molecular biomarker discovery and progress. Mol Cancer 2007; 6: 1.

[2] Lee AWM, Ng WT, Chan JYW, Corry J, Makitie A, Mendenhall WM, Rinaldo A, Rodrigo JP, Saba NF, Strojan P, Suarez C, Vermorken JB, Yom SS and Ferlito A. Management of locally recurrent nasopharyngeal carcinoma. Cancer Treat Rev 2019; 79: 101890.

[3] Yuan JM, Wang XL, Xiang YB, Gao YT, Ross RK and Yu MC. Preserved foods in relation to risk of nasopharyngeal carcinoma in Shanghai, China. Int J Cancer 2000; 85: 358-363.

[4] Huang T, Ploner A, Chang ET, Liu Q, Cai Y, Zhang Z, Chen G, Huang Q, Xie S, Cao S, Jia W, Zheng Y, Liao J, Chen Y, Lin L, Ernberg I, Huang G, Zeng Y, Zeng Y, Adami HO and Ye W. Dietary patterns and risk of nasopharyngeal carcinoma: a population-based case-control study in southern China. Am J Clin Nutr 2021; 114: 462-471.

[5] Ward MH, Pan WH, Cheng YJ, Li FH, Brinton LA, Chen CJ, Hsu MM, Chen IH, Levine PH, Yang CS and Hildesheim A. Dietary exposure to nitrite and nitrosamines and risk of nasopharyngeal carcinoma in Taiwan. Int J Cancer 2000; 86: 603-609.

[6] Gallicchio L, Matanoski G, Tao XG, Chen L, Lam TK, Boyd K, Robinson KA, Balick L, Mickelson S, Caulfield LE, Herman JG, Guallar E and Alberg AJ. Adulthood consumption of preserved and nonpreserved vegetables and the risk of nasopharyngeal carcinoma: a systematic review. Int J Cancer 2006; 119: 1125-1135.

[7] Zheng X, Luo Y, Christensson B and Drettner B. Induction of nasal and nasopharyngeal tumours in Sprague-Dawley rats fed with Chinese salted fish. Acta Otolaryngol 1994; 114: 98-104.

[8] Li Y, Lu J, Peng Z, Tan G, Liu N, Huang D, Zhang Z, Duan C, Tang X and Tang F. N,N'-dinitrosopiperazine-mediated AGR2 is involved in metastasis of nasopharyngeal carcinoma. PLoS One 2014; 9: e92081.

[9] Tang FQ, Duan CJ, Huang DM, Wang WW, Xie CL, Meng JJ, Wang L, Jiang HY, Feng DY, Wu SH, Gu HH, Li MY, Deng FL, Gong ZJ, Zhou H, Xu YH, Tan C, Zhang X and Cao Y. HSP70 and mucin 5B: novel protein targets of N,N'-dinitrosopiperazine-induced nasopharyngeal tumorigenesis. Cancer Sci 2009; 100: 216-224.

[10] Li Y, Lu J, Zhou S, Wang W, Tan G, Zhang Z, Dong Z, Kang T and Tang F. Clusterin induced by N,N'-Dinitrosopiperazine is involved in nasopharyngeal carcinoma metastasis. Oncotarget 2016; 7: 5548-5563.

[11] Lee JH, Xiong F and Li W. Enhancer RNAs in cancer: regulation, mechanisms and therapeutic potential. RNA Biol 2020; 17: 1550-1559.

[12] Whyte WA, Orlando DA, Hnisz D, Abraham BJ, Lin CY, Kagey MH, Rahl PB, Lee TI and Young RA. Master transcription factors and mediator establish super-enhancers at key cell identity genes. Cell 2013; 153: 307-319.

[13] Li W, Notani D and Rosenfeld MG. Enhancers as non-coding RNA transcription units: recent insights and future perspectives. Nat Rev Genet 2016; 17: 207-223.

[14] Castillo-Guzman D and Chedin F. Defining R-loop classes and their contributions to genome instability. DNA Repair (Amst) 2021; 106: 103182.

[15] Pefanis E, Wang J, Rothschild G, Lim J, Kazadi D, Sun J, Federation A, Chao J, Elliott O, Liu ZP, Economides AN, Bradner JE, Rabadan R and Basu U. RNA exosome-regulated long non-coding RNA transcription controls super-enhancer activity. Cell 2015; 161: 774-789.

[16] Chen H, Li C, Peng X, Zhou Z, Weinstein JN; Cancer Genome Atlas Research Network, Liang H. A pan-cancer analysis of enhancer expression in nearly 9000 patient samples. Cell 2018; 173: 386-399, e12.

[17] Zhang X, Pang P, Jiang M, Cao Q, Li H, Xu Y, Li Y, Chen X and Han J. eRNAs and superenhancer lncRNAs are functional in human prostate cancer. Dis Markers 2020; 2020: 8847986.

[18] Zhou W, Huang K, Zhang Q, Ye S, Zhong Z, Zeng C, Peng G, Li L and Ye Q. LINC00844 promotes proliferation and migration of hepatocellular carcinoma by regulating NDRG1 expression. PeerJ 2020; 8: e8394.

[19] Zhao T, Meng Y, Wang Y and Wang W. NDRG1 regulates osteosarcoma cells via mediating the mitochondrial function and CSCs differentiation. J Orthop Surg Res 2021; 16: 364.

[20] Park KC, Paluncic J, Kovacevic Z and Richardson DR. Pharmacological targeting and the diverse functions of the metastasis suppressor, NDRG1, in cancer. Free Radic Biol Med 2020; 157: 154-175.

[21] Guo DD, Xie KF and Luo XJ. Hypoxia-induced elevated NDRG1 mediates apoptosis through reprograming mitochondrial fission in HCC. Gene 2020; 741: 144552.

[22] Wang Y, Zhou Y, Tao F, Chai S, Xu X, Yang Y, Yang Y, Xu H and Wang K. N-myc downstream regulated gene 1(NDRG1) promotes the stem-like properties of lung cancer cells through stabilized c-Myc. Cancer Lett 2017; 401: 53-62.

[23] Li A, Zhu X, Wang C, Yang S, Qiao Y, Qiao R and Zhang J. Upregulation of NDRG1 predicts poor outcome and facilitates disease progression by influencing the EMT process in bladder cancer. Sci Rep 2019; 9: 5166.

[24] Aikemu B, Shao Y, Yang G, Ma J, Zhang S, Yang X, Hong H, Yesseyeva G, Huang L, Jia H, Wang C, Zang L, Sun J and Zheng M. NDRG1 regulates filopodia-induced colorectal cancer invasiveness via modulating CDC42 activity. Int J Biol Sci 2021; 17: 1716-1730.

[25] Quan Y, Cui Y, Wahafu W, Liu Y, Ping H and Zhang X. MLL5α activates AR/NDRG1 signaling to suppress prostate cancer progression. Am J Cancer Res 2020; 10: 1608-1629.

[26] Cen G, Zhang K, Cao J and Qiu Z. Downregulation of the N-myc downstream regulated gene 1 is related to enhanced proliferation, invasion and migration of pancreatic cancer. Oncol Rep 2017; 37: 1189-1195.

[27] Chang X, Xu X, Xue X, Ma J, Li Z, Deng P, Chen J, Zhang S, Zhi Y and Dai D. NDRG1 controls gastric cancer migration and invasion through regulating MMP-9. Pathol Oncol Res 2016; 22: 789-796.

[28] Hu ZY, Xie WB, Yang F, Xiao LW, Wang XY, Chen SY and Li ZG. NDRG1 attenuates epithelial-mesenchymal transition of nasopharyngeal cancer cells via blocking Smad2 signaling. Biochim Biophys Acta 2015; 1852: 1876-1886.

[29] Park A, Oh S, Jung KL, Choi UY, Lee HR, Rosenfeld MG and Jung JU. Global epigenomic analysis of KSHV-infected primary effusion lymphoma identifies functional MYC superenhancers and enhancer RNAs. Proc Natl Acad Sci U S A 2020; 117: 21618-21627.

[30] Zhuo W, Liu Y, Li S, Guo D, Sun Q, Jin J, Rao X, Li M, Sun M, Jiang M, Xu Y, Teng L, Jin Y, Si J, Liu W, Kang Y and Zhou T. Long noncoding RNA GMAN, up-regulated in gastric cancer tissues, is associated with metastasis in patients and promotes translation of ephrin A1 by competitively binding GMAN-AS. Gastroenterology 2019; 156: 676-691, e611.

[31] Pan CW, Wen S, Chen L, Wei Y, Niu Y and Zhao Y. Functional roles of antisense enhancer RNA for promoting prostate cancer progression. Theranostics 2021; 11: 1780-1794.

[32] Zhao Y, Zhou J, He L, Li Y, Yuan J, Sun K, Chen X, Bao X, Esteban MA, Sun H and Wang H.

MyoD induced enhancer RNA interacts with hnRNPL to activate target gene transcription during myogenic differentiation. Nat Commun 2019; 10: 5787.
[33] Yuan M, Zhang X, Zhang J, Wang K, Zhang Y, Shang W, Zhang Y, Cui J, Shi X, Na H, Fang D, Zuo Y and Ren S. DC-SIGN-LEF1/TCF1-miR-185 feedback loop promotes colorectal cancer invasion and metastasis. Cell Death Differ 2020; 27: 379-395.
[34] Zhou Y, Xu S, Zhang M and Wu Q. Systematic functional characterization of antisense eRNA of protocadherin α composite enhancer. Genes Dev 2021; 35: 1383-1394.
[35] Luo H, Zhu G, Eshelman MA, Fung TK, Lai Q, Wang F, Zeisig BB, Lesperance J, Ma X, Chen S, Cesari N, Cogle C, Chen B, Xu B, Yang FC, So CWE, Qiu Y, Xu M and Huang S. HOTTIP-dependent R-loop formation regulates CTCF boundary activity and TAD integrity in leukemia. Mol Cell 2022; 82: 833-851, e811.
[36] Huang J, Li J, Li Y, Lu Z, Che Y, Mao S, Lei Y, Zang R, Zheng S, Liu C, Wang X, Li N, Sun N and He J. Interferon-inducible lncRNA IRF1-AS represses esophageal squamous cell carcinoma by promoting interferon response. Cancer Lett 2019; 459: 86-99.
[37] Hajmirza A, Emadali A, Gauthier A, Casasnovas O, Gressin R and Callanan MB. BET family protein BRD4: an emerging actor in NFκB signaling in inflammation and cancer. Biomedicines 2018; 6: 16.
[38] Donati B, Lorenzini E and Ciarrocchi A. BRD4 and cancer: going beyond transcriptional regulation. Mol Cancer 2018; 17: 164.
[39] Li Z, Boone D and Hann SR. Nucleophosmin interacts directly with c-Myc and controls c-Myc-induced hyperproliferation and transformation. Proc Natl Acad Sci U S A 2008; 105: 18794-18799.
[40] Ginno PA, Lott PL, Christensen HC, Korf I and Chedin F. R-loop formation is a distinctive characteristic of unmethylated human CpG island promoters. Mol Cell 2012; 45: 814-825.
[41] Niehrs C and Luke B. Regulatory R-loops as facilitators of gene expression and genome stability. Nat Rev Mol Cell Biol 2020; 21: 167-178.
[42] Li W, Notani D, Ma Q, Tanasa B, Nunez E, Chen AY, Merkurjev D, Zhang J, Ohgi K, Song X, Oh S, Kim HS, Glass CK and Rosenfeld MG. Functional roles of enhancer RNAs for oestrogen-dependent transcriptional activation. Nature 2013; 498: 516-20.
[43] Jiao W, Chen Y, Song H, Li D, Mei H, Yang F, Fang E, Wang X, Huang K, Zheng L and Tong Q. HPSE enhancer RNA promotes cancer progression through driving chromatin looping and regulating hnRNPU/p300/EGR1/HPSE axis. Oncogene 2018; 37: 2728-2745.
[44] Ariel F, Lucero L, Christ A, Mammarella MF, Jegu T, Veluchamy A, Mariappan K, Latrasse D, Blein T, Liu C, Benhamed M and Crespi M. R-Loop mediated trans action of the APOLO long noncoding RNA. Mol Cell 2020; 77: 1055-1065, e1054.
[45] Gibbons HR, Shaginurova G, Kim LC, Chapman N, Spurlock CF 3rd and Aune TM. Divergent lncRNA GATA3-AS1 regulates GATA3 transcription in T-helper 2 cells. Front Immunol 2018; 9: 2512.
[46] Box JK, Paquet N, Adams MN, Boucher D, Bolderson E, O'Byrne KJ and Richard DJ. Nucleophosmin: from structure and function to disease development. BMC Mol Biol 2016; 17: 19.
[47] Okuwaki M. The structure and functions of NPM1/Nucleophsmin/B23, a multifunctional nucleolar acidic protein. J Biochem 2008; 143: 441-448.
[48] Xu DH, Liu F, Li X, Chen XF, Jing GJ, Wu FY, Shi SL and Li QF. Regulatory role of nucleophosmin during the differentiation of human liver cancer cells. Int J Oncol 2014; 45: 264-272.
[49] Li Z and Hann SR. The Myc-nucleophosmin-ARF network: a complex web unveiled. Cell Cycle 2009; 8: 2703-2707.
[50] Qin G, Wang X, Ye S, Li Y, Chen M, Wang S, Qin T, Zhang C, Li Y, Long Q, Hu H, Shi D, Li J, Zhang K, Zhai Q, Tang Y, Kang T, Lan P, Xie F, Lu J and Deng W. NPM1 upregulates the transcription of PD-L1 and suppresses T cell activity in triple-negative breast cancer. Nat Commun 2020; 11: 1669.
[51] Gallo A, Lo Sterzo C, Mori M, Di Matteo A, Bertini I, Banci L, Brunori M and Federici L. Structure of nucleophosmin DNA-binding domain and analysis of its complex with a G-quadruplex sequence from the c-MYC promoter. J Biol Chem 2012; 287: 26539-26548.